Graphene–Gold Metasurface Architectures for Ultrasensitive Plasmonic Biosensing

*Shuwen Zeng, Kandammathe Valiyaveedu Sreekanth, Jingzhi Shang, Ting Yu, Chih-Kuang Chen, Feng Yin, Dominique Baillargeat, Philippe Coquet, Ho-Pui Ho, Andrei V. Kabashin, and Ken-Tye Yong**

With spectacular progress of surface plasmon resonance and localized plasmon resonance–based sensing modalities for last years, plasmonic biosensing has become the core label-free technology for studies of biomolecular interactions.[1,2] Despite a series of advantages offered by direct, label-free detection, plasmonic technology still needs a drastic improvement of sensitivity to match requirements of many critical areas of biomedical research, including early disease diagnostics and pharmacology.[3–5] Here, we describe novel hybrid graphene/gold metasurface architectures for plasmon excitation, which can provide a significant gain in sensitivity and give access to the detection of trace amounts of target analytes. Benefiting from extreme singularities in phase of reflected light as a result of plasmon field enhancement on the graphene sheet and a strong plasmon-mediated energy confinement, the metasurface demonstrates much improved sensitivity to refractive index variations nearby and to the attachment of signal-enhancing Au nanoparticle (NP) tags. Running a protocol of single-stranded DNA (ssDNA) on graphene/gold metasurface, we report the sensitivity of 1×10^{-18} M, which is three orders of magnitude higher than any state-of-the-art plasmonic sensors. Combined with the ability of graphene-based substrate to selectively absorb some molecules through pi-stacking forces, the proposed metasurface architecture provides a unique platform to selectively detect aromatic rings structure biomolecules (e.g., DNA, RNA, peptides, and cytokines). Our proof-of-concept results offer a pathway toward simple and scalable technology for the detection of trace amounts of analytes.

Surface plasmons are oscillations of free electrons in metals, which exist at the metal–dielectric interface and can be optically excited over thin metal films and nanostructures.[1–3] Electric field associated with these oscillations decays exponentially into the dielectric medium making plasmons extremely sensitive to refractive index of this medium. This remarkable property has been employed in surface plasmon resonance (SPR) biosensors,[4–6] which rely on the control of biological binding/recognition events on a thin gold film via refractive index monitoring. The attachment of the target analyte to a gold-supported receptor causes a perturbation of plasmon electric field, which is normally monitored by following angular or spectral position of the plasmon-related feature in reflected light. Similar effect can be obtained with localized plasmons over metal nanostructures in conditions of localized plasmon resonance (LPR).[3,7] It is important that both modalities can avoid expensive, time-consuming, and precision-interfering labeling steps to mark analytes, while their high sensitivity is due to strong plasmon-related probing field and a resonant nature of its response. Despite significant progress for last couple of decades, both modalities of plasmonic sensors still need a drastic improvement of sensitivity to compete with classical labeling approaches. The detection limit of SPR biosensors in terms of the amount of a biomaterial accumulated on the surface is of

Dr. S. Zeng, Prof. D. Baillargeat, Prof. P. Coquet, Prof. K.-T. Yong
CINTRA CNRS/NTU/THALES
UMI 3288
Research Techno Plaza
50 Nanyang Drive, Border X Block, Singapore 637553, Singapore
E-mail: ktyong@ntu.edu.sg

Dr. S. Zeng, Dr. F. Yin, Prof. K.-T. Yong
School of Electrical and Electronic Engineering
Nanyang Technological University
Singapore 639798, Singapore

Dr. K. V. Sreekanth, Dr. J. Shang, Prof. T. Yu
Division of Physics and Applied Physics
School of Physical and Mathematical Sciences
Nanyang Technological University
21 Nanyang Link, Singapore 637371, Singapore

Dr. C.-K. Chen
The Polymeric Biomaterials Lab
Feng Chia University
Taichung 40724, Taiwan

Prof. D. Baillargeat
XLIM UMR CNRS 7252
Université de Limoges/CNRS
Limoges 87060, France

Prof. P. Coquet
Institut d'Electronique
de Microélectronique et de Nanotechnologie (IEMN)
CNRS UMR 8520 – Université de Lille 1
59650 Villeneuve d'Ascq, France

Prof. H.-P. Ho
Department of Electronic Engineering
The Chinese University of Hong Kong
Hong Kong, 999077

Prof. A. V. Kabashin
Aix Marseille University
CNRS, LP3 UMR 7341
Campus de Luminy
163 Avenue de Luminy, Case 917, 13288 Marseille cedex 9, France

DOI: 10.1002/adma.201501754

the order of 1 pg mm^{-2} (for LPR biosensors the relevant value is about 1000 pg mm^{-2}) that is inferior by two orders of magnitude to labeling methods.[6,8] As an example, current SPR setups are not able to detect low molecular weight molecules such as DNA, cytokine, and hormones especially at concentration below 1×10^{-15} M, which is 1–2 orders of magnitude higher than required in many tasks of early-stage disease diagnostics.[8,9]

Such a lack in the detection limit compared to classical labeling methods can be gained up by passing from amplitude to phase characteristics of light.[10–12] As phase is not determined in the point where reflected intensity is equal to zero (point of darkness),[13] it can experience a sharp jump under SPR and this jump can be employed as a sensing parameter. Here, a much superior phase sensitivity compared to the amplitude one is largely due to field intensity factor: the phase jump takes place in the very minimum of the SPR curve where probing electric field is maximal while relevant change of amplitude characteristics occurs in its slopes where probing field is much weaker.[13] In this case, lower in the intensity of light at the point of resonance (darker is the structure), stronger is the probing field and sharper is the phase jump. Although Fresnel's formulae predict infinite Heaviside-like phase behavior under a proper selection of gold film thickness under SPR,[13] this singularity never happens in practice due to nonzero film roughness and the reflected intensity inside the dip is normally not lower than 3%–5%. One of solutions of this problem of conventional materials consists in involving metamaterials, or artificial materials composed of properly arranged metal nanodots (meta-atoms) with nanoscale distance between them, which can provide controlled photonic response or new sensing functionalities.[2,14] It has been recently shown that a proper design of metamaterial supporting diffraction-coupled plasmons can lead to complete darkness, yielding to extreme phase singularities.[7] The employment of such phase singularities opens up access to single molecular label-free detection with spectacular opportunities for the improvement of current state-of-the-art biosensing technology.[7]

Here, we explore other routes to implement improved phase sensitivity and focus our attention to graphene plasmonics.[15–19] It has been recently shown that the presence of graphene layers on gold can result in an improved sensing response in conventional SPR and opens access to new functionalization strategies through pi-stacking interactions.[20–22] We show that graphene plasmonics structures can provide extreme phase features as a result of electric field enhancement, offering much improved phase sensitivity. We additionally consider graphene plasmonics architecture with gold nanoparticle–based enhancement to further improve the sensing response.[23] The recorded sensitivity of 1×10^{-18} M for detecting ssDNA appears to be far beyond relevant values for any state-of-the-art plasmonic sensors available in the markets and bench side prototypes.[5,6,24] Presenting an Au-perturbed single layer honeycomb lattice of C atoms, the graphene–gold interface fits the definition of "metasurfaces" to provide a drastic concentration of plasmon electric field in 2D plane as a novel functionality.[25,26]

In the basic geometry, the proposed metasurface architecture consists of a gold film coated by a single (or multi) sheets of graphene, as shown in **Figure 1**a. The layer/layers of graphene is/are deposited in such a way that graphene and gold are in full electric contact. In another gold nanoparticle–enhanced geometry, spherical Au nanoparticles are additionally employed as amplification tags to enhanced SPR sensing response, as shown in Figure 1b. Both cases imply the excitation of surface plasmon polaritons over the graphene–gold interface that can be done, e.g., with a prism coupling scheme using the Kretschmann–Raether arrangement (Figure 1a,b). Under the production of surface plasmon resonance, the distribution of electric field is characterized by an exponential decay toward both gold film and adjacent dielectric medium, respectively. In this case, the presence of graphene sheets leads to a strong localization of the field at the graphene–gold interface, as shown in Figure 1c, and a drastic field enhancement. Figure 1e illustrates the field enhancement effect under the deposition of different numbers of graphene layers on the gold surface. It is visible that more than fourfold enhancement of electric field takes place under the deposition of a single graphene layer on gold, while a further deposition of layers (two ones and more) does not provide the field enhancement effect. **Figure 2**a illustrates the behavior of amplitude and phase parameters of light reflected under SPR. One can see that phase experiences a sharp "Heaviside-like" singularity in the very minimum of the SPR curve (point of light "darkness"),[7] where the probing electric field is maximum. It is worth noting that the conventional SPR detection method based on the angular measurement is strongly dependent on the plasmon damping of the graphene layers due to their absorbing dielectric property. In this case, the signal change (i.e., the resonance angle change) to the surrounding environment increases with the number of graphene layers.[20] However, more graphene layers would result in electron energy loss of the excited SPR electric field. This will increase the full width at half maximum (FWHM) of the SPR curves and thus significantly reduce the SPR detection resolution.[20,27] For the phase detection approach, the signal change (i.e., the phase jump at the resonance angle) is only dependent on the minimum reflectivity of the SPR curves. Thus, when the value of the minimum reflectivity is lowered, the change of the phase signal becomes larger. When the reflectivity has the lowest value, the intensity of the excited electric field will reach a maximum value which means that almost all the incident light energy (≈100%) has been successfully transferred to the resonance energy of the SPR waves. As shown in Figure 2b, the response of phase to variations of refractive index of the adjacent dielectric medium appears to be directly proportional to the intensity of the probing field at the graphene–gold interface: it is more than fourfold enhanced when single layer of graphene is deposited on the gold surface, while the deposition of two and more graphene layers does not improve the resulting sensitivity. An additional employment of Au tags (Figure 1b) leads to a further local enhancement of probing electric at the point of their attachment of the metasurface and this event leads to a local redistribution of electric field pattern (Figure 1d). In our analysis, we also examined local electric field enhancement due to the attachment of gold nanoparticles of different sizes. We found that the best 40-fold enhancement takes place when 30 nm nanoparticles are used (Figures S3 and S4, Supporting Information): this effect is attributed to the highest absorption efficiency and lowest scattering efficiency of

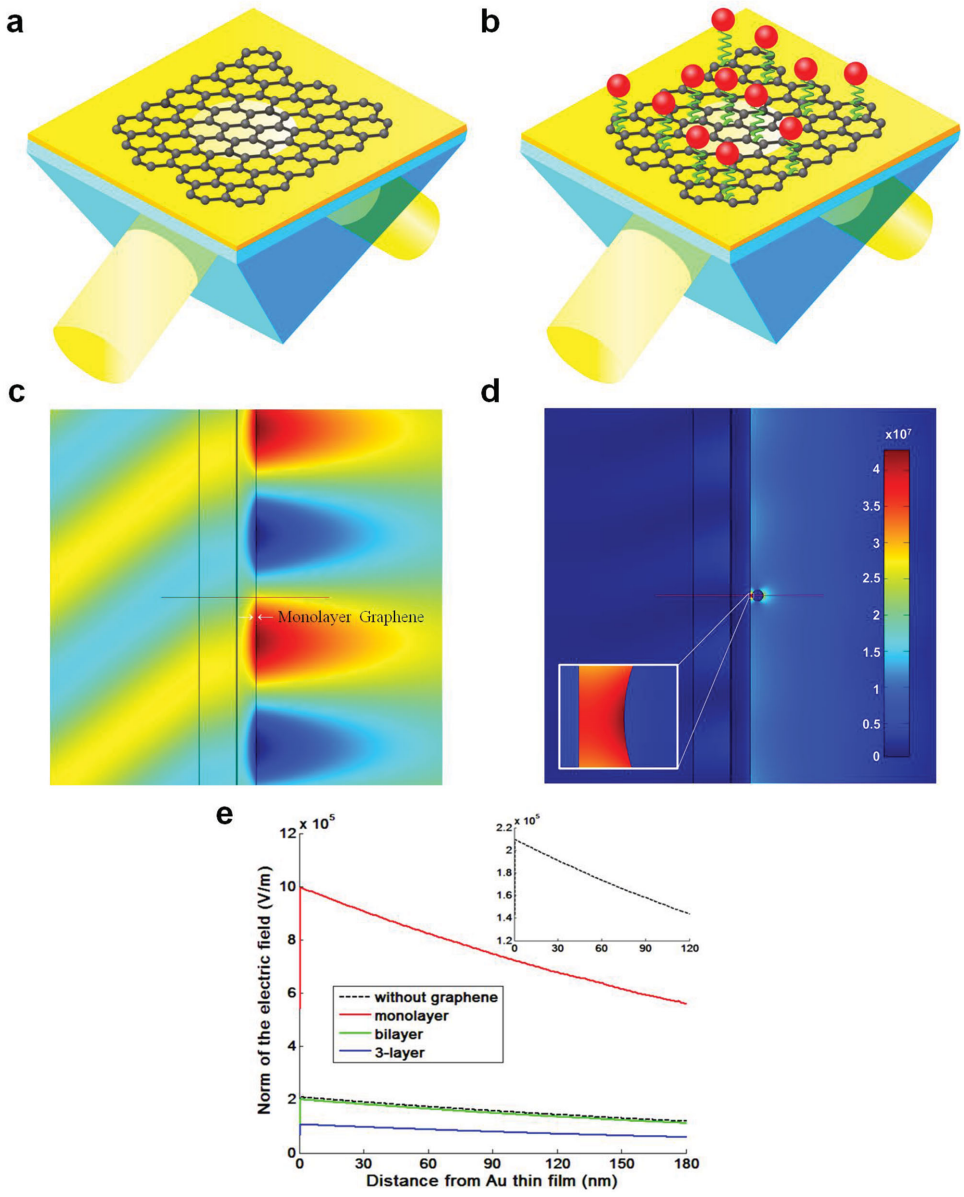

Figure 1. Designs of graphene–gold metasurface architectures. a) Basic architecture with a layer of graphene deposited on the gold surface. To excite surface plasmon polariton over the graphene–gold interface, a light beam is typically passed through a glass prism and reflected from a 50 nm gold film deposited on one of its facets. b) Advanced nanoparticle-enhanced architecture with the employment of Au nanoparticles as SPR amplification tags. c) Finite element analysis (FEA) simulations of resonant monolayer graphene-coated Au sensing film: Electric field in *y*-component, showing angle of incident light ≈52° and clear evanescent field at the sensing interface. d) FEA simulations of resonant spherical Au NP coupling to the monolayer graphene-coated Au sensing film: Norm of the electric filed with Au NP (diameter is 30 nm, distance from the sensing film is 5 nm). e) Cross-section plots for total electric fields along $y = 0$ with different number of graphene layers L.

the 30 nm Au nanoparticle when they are coupled to the graphene-coated Au thin film.[28] Giovannetti et al. reported that electrons would transfer from graphene to the surface of Au thin film in order to maintain the continuity of the Fermi levels when they contact with each other, as the work function of Au (5.54 eV) is larger than that of graphene (4.5 eV).[29] Therefore, the charge transfer is one of the main reasons for the SPR field enhancement which is induced by the graphene layers. Moreover, the excited plasmons at the graphene surface have a sensitive response toward the effective dielectric constant change of the surrounding environment. And all these factors contributed to the strong enhancement in the detection sensitivity of our proposed sensing system. Single graphene layer is also known to absorb 2.3% of transmitted light and lead to a certain loss of light intensity,[30,31] which could explain the decrease of SPR sensitivity and field intensity when the number of graphene layers coated on the Au sensing film is larger than 2.

To confirm the consistency of the proposed concept and the validity of our calculations, we fabricated a monolayer graphene–coated Au sensing film and compared its sensing

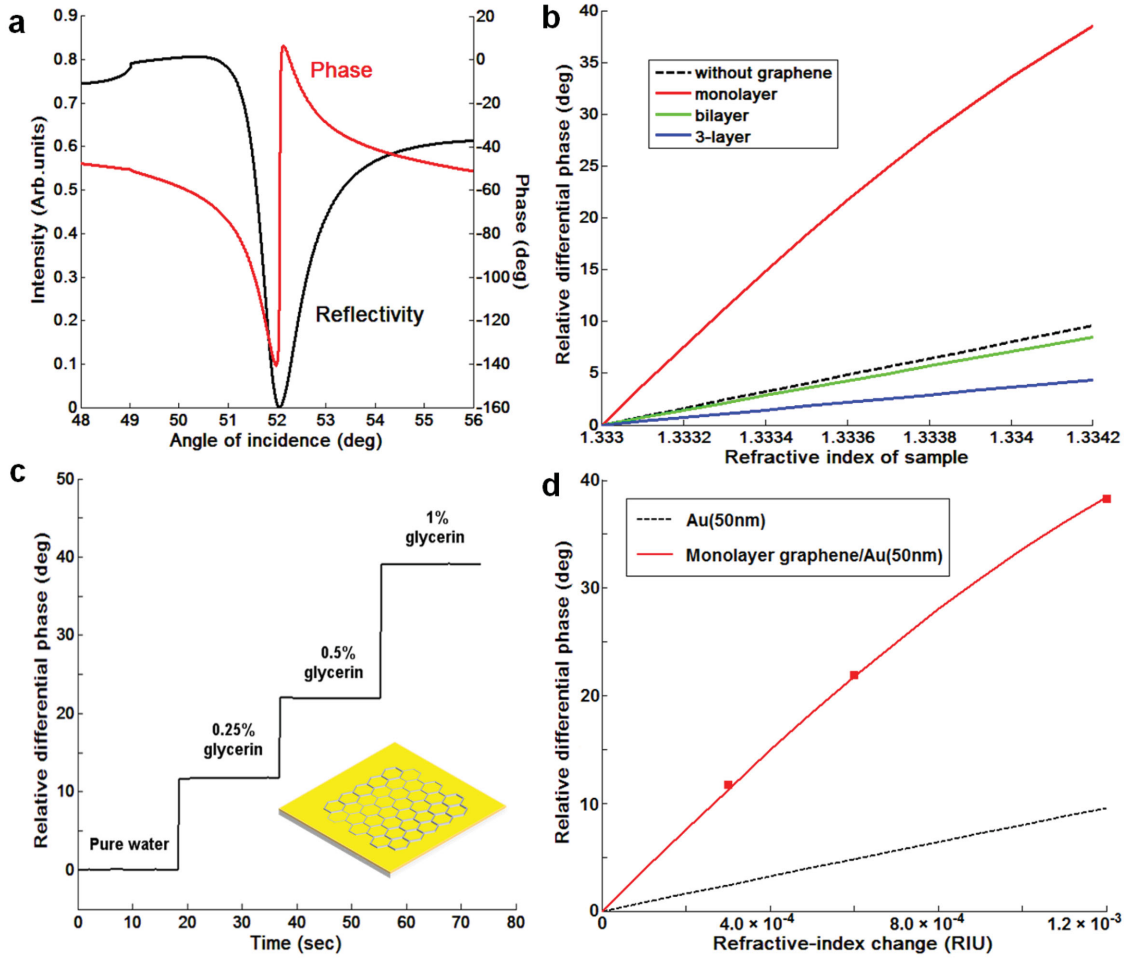

Figure 2. Assessment of phase sensitivity of graphene–gold metamaterial to refractive index variations. a) Calculated reflectivity (black) and phase (red) of light as functions of the angle of light incidence of the gold–graphene interface, corresponding to maximum probing field. Phase experiences a sharp singularity in the minimum of SPR curve. b) Response of phase due to the adsorption of biomolecules with different number of graphene layers *L*. c) real-time differential phase measurement for various weight ratios of glycerin in water using monolayer graphene-coated Au thin film as sensing substrate. The baseline was measured after flowing deionized (DI) water onto the sensor surface. d) Comparison of calibration curves for graphene-coated gold film and pure Au film substrates under changes of the refractive index in the environment. All lines in the figure are theoretical analyses. The square symbols correspond to experimental measurements in (c).

performance with that of the bare Au thin film by using a home-built differential phase–sensitive SPR sensor (see details in Section 2.3, Supporting Information). The large area monolayer graphene (≈1.5 cm × 1.5 cm) was grown on a high-purity copper foil by using a low-pressure chemical vapor deposition method and it was transferred from the copper substrate to a 50 nm Au thin film. A 2.5 nm layer of Ti was placed between the Au film and the glass substrate in order to improve the adhesion of gold. Aqueous solutions of glycerin with different weight ratios were pumped into the SPR flow cell and interacted with the monolayer graphene–coated Au thin film and bare Au thin film, respectively. Figure 2c shows the responses of phase to a gradual increase of concentration of glycerin: 0.25%, 0.5%, and 1%. It is visible that in this range of chosen concentrations phase response is directly proportional to the concentration, while a relatively low level of experimental noises illustrates the potential of the chosen phase-sensitive instrumental scheme for achieving relatively low detection limit values. Figure 2d compares phase responses of graphene-coated and pure Au film to refractive index variations, as calculated from the glycerin calibration measurements. One can see that both geometries evidence a gradual linear change of phase under the increase of refractive index. Such signal changes become saturated when the shift of refractive index is larger than 10^{-3} refractive index unit (RIU). However, the phase response of graphene–gold metasurface geometry appears to be about four times stronger compared to the pure gold film case, which is in excellent agreement with our theoretical estimations of sensitivity and field enhancement gains, as shown in Figures 2b and 1e, respectively. As it has been experimentally shown,[10,12,13] the employment of phase as a sensitive parameter can lead to the detection limit as low as 10^{-8} RIU that is more than one order of magnitude better compared to conventional SPR employing amplitude parameters (resonant angle of incidence or wavelength). Therefore, the reported four times increase of sensitivity through the employment of

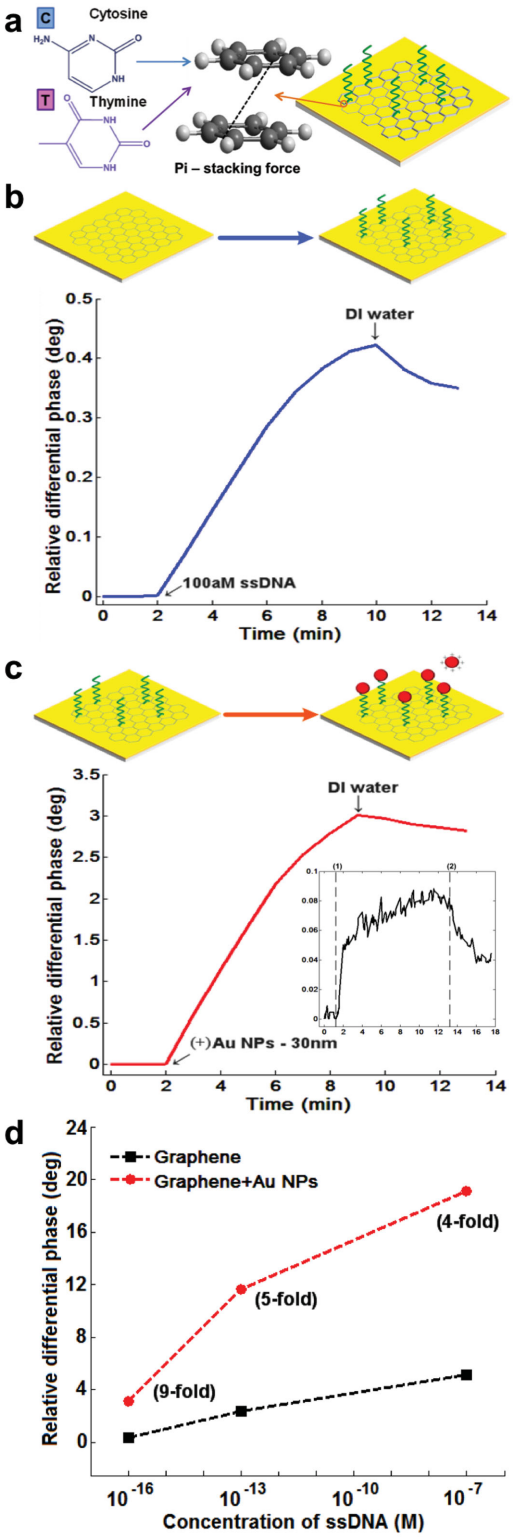

Figure 3. Detection of low-concentration ssDNA by biosensor employing graphene–gold metasurface architectures. a) Schematics of binding ssDNA to monolayer graphene-coated Au thin film by pi-stacking interaction; response curves obtained after flowing solutions of b) ssDNA with concentration of 100×10^{-18} M and c) positive-charged Au NPs with 30 nm in diameter (OD = 1.0), followed by deionized (DI) water. The baselines were measured b) after flowing DI water and c) binding of 100×10^{-18} M ssDNA onto the sensor surface; the inset in (c) shows the absence of any unspecific binding between positive-charged Au NPs and bare monolayer graphene-coated sensing film while injecting solutions of positive-charged Au NPs with 30 nm diameter (OD = 1.0) (1) and DI water (2). d) Response and magnitude of enhancement (in the bracket) obtained with (circles) and without (squares) exposing the monolayer graphene-coated sensing film to positive-charged Au NPs after ssDNA.

graphene–gold architecture opens up the possibility for lowering of the detection limit of phase-sensitive SPR down to 10^{-9} RIU, which promises the detection of trace amounts of biomolecules down to single molecular level.[7] It should be noted that due to the employment of phase as a sensing parameter our sensitivity is far beyond all values reported with graphene-enhanced SPR sensing schemes.[16,18,20,32] In general, the proposed graphene–gold metasurface architecture offers a very efficient approach for the implementation of extreme phase singularities. Similar effect was recently recorded using gold nanodot array–based metamaterials based on diffraction coupling of localized plasmons.[7] Both approaches reveal a drastic sharpening of phase features due to the enhancement of electric field intensity in the sensing interface. As it was shown in ref. [7], this phenomenon is accompanied by near-zero intensity reflection (light darkness).

It is important that the proposed graphene–gold metasurface–based biosensing approach offers novel surface chemistry functionalization strategies, which can provide decisive advantages over conventional SPR for many biosensing tasks. In particular, aromatic ring structure biomolecules such as helical peptides or proteins can selectively bind to the surface of graphene due to pi-stacking interactions,[21,22] as illustrated in **Figure 3**a, whereas conventional SPR sensors that use bare Au sensing film requires tedious surface functionalization steps to accomplish the same task. To assess the efficiency of such functionalization strategy, we tested the proposed metasurface architecture in a model of single-stranded DNA, which can adsorb on graphene through the pi-stacking interactions: this mechanism renders possible a much more efficient binding of ssDNA to graphene compared to double-stranded DNA.[22] In our tests, we pumped 7.3 kDa 24-mer ssDNA solutions of different concentrations ranging from 100×10^{-18} to 100×10^{-9} M into a flow cell contacting with the graphene–gold metasurface (Section 2.3.3, Supporting Information). The size of our flow chamber is 1.5 cm × 1.5 cm × 0.5 cm and the diameter of 785 nm laser spot is 1 mm. The solutions containing ssDNA molecules were injected into the chamber from the bottom and once the chamber was filled up, the injection was stopped to allow a complete interaction to take place between the ssDNA molecules and the graphene-coated sensing film. The laser spot was focused at the center of the interaction area. Each time before injection, a calibration process as shown in Figure 2c was carried out to check and confirm the quality of the monolayer graphene–coated sensing substrate. As shown in Figure 3b and Figures S8 and S9 (Supporting Information), we could observe phase signal changes upon introducing the ssDNA solutions onto the sensor head, which corresponded to the binding of ssDNA on the monolayer graphene–coated sensing substrates. After 8 min reaction time, deionized (DI) water was

injected into the system to remove any unbound and weakly attached ssDNA and this step resulted in a slight decrease and stabilization of the signal. Longer immersion time did not affect the signal change. To further improve the SPR sensitivity, we used an additional step, which implies the employment of Au nanoparticles to enhance the resulting signal (Figure 1b). Solutions containing positive-charged 30 nm Au NPs of identical optical density (OD) were supplied onto the ssDNA-modified sensing substrate. Since zeta potential of desalted ssDNA solution was measured to be negative, strong electrostatic bindings occurred when they interacted with the positively charged Au NPs. After a few minutes of reaction time, DI water was again used to flush away "free" Au NPs, while the attached Au NPs left on the ssDNA-modified sensing film. In this case, graphene, ssDNA, and Au NPs formed a sandwich structure on the Au film substrate, which resulted in a strong change in the overall SPR signal (Figure 3c). In a control test, Au nanoparticles were supplied under same conditions without the ssDNA adsorption step. However, we did not record any significant change of the phase signal (inset to Figure 3c), which evidenced the absence of any affinity between the positively charged nanoparticles and graphene-coated gold. Figure 3d summarizes the signal enhancement factors under different concentrations of ssDNA. One can see that the largest enhancement was obtained for ssDNA solutions with 100×10^{-18} M, while higher concentrations (100×10^{-15} to 100×10^{-9} M) led to slightly lower enhancement factors. Such decrease of enhancement under high concentration can be explained by the saturation of SPR signal due to a complete coverage of ssDNA within the light spot area (1 mm × 1 mm) of the sensing film. It should be noted that observed nanoparticle-based enhancement factors are in good agreement with our numerical analysis (Figures S3 and S4, Supporting Information).

To summarize the obtained data, when used with Au amplification tags, the graphene–gold biosensing structure provided the detection limit of 1×10^{-18} M for 7.3 kDa 24-mer ssDNA at a signal-to-noise ratio of 3:1, which is higher than the detection limit reported for not only current state-of-the-art graphene-based SPR biosensor (human IgG of 150 kDa, 0.5×10^{-9} M, ref. [32] and Au NP–enhanced phase-sensitive SPR techniques (TNF-α of 17 kDa, 0.03×10^{-12} M, ref. [23], but also gold nanorod–enhanced localized SPR sensors (streptavidin of 53 kDa, 10×10^{-9} M, ref. [3] and even nanomechanical biosensors (25-mer ssDNA of 7.6 kDa, 500×10^{-18} M, ref. [33]. The recorded sensitivity evidence a huge potential of the graphene–gold metasurface architectures for detecting many other aromatic ring structure biomolecules (toxins, vitamins, cancer biomarkers, etc.) for which conventional SPR is not sensitive enough. We envision that a proper functionalization of Au nanoparticles by complementary counterparts of targeted biomolecules will further improve the bioselectivity of our engineered sensing configuration.[34]

In summary, the designed novel graphene–gold metasurface–based biosensing architectures make possible extreme phase singularities due to a strong field enhancement on the graphene–gold interface. Profiting from these singularities, we recorded four times increase of sensitivity compared to phase-sensitive SPR and another order of magnitude gain of sensitivity by employing nanoparticle-based enhancement of phase signals. One of huge advantages of the proposed architectures over conventional plasmonic biosensing consists in the possibility of involvement of strong pi-stacking forces in the development of functionalization strategies using many aromatic structure biomolecules (helical peptides, proteins, ssDNA, etc.). For the conventional SPR detection using plain gold film, it is generally required to functionalize the gold sensing surface with capture molecules to enhance the adsorption efficiency before performing any measurement for detecting the targeted samples. For our sensing experiments here that uses graphene-coated film, we could achieve directly label-free ssDNA detection through the pi-stacking interaction between graphene and ssDNA without the need of any modification steps for preparing "activated" sensing film. As an example, we illustrated at least three orders gain in sensitivity by using a model of ssDNA adsorption on graphene–gold metasurface. Our system was subjected to continue evaluation for six months for determining the setup stability and showed same reproducibility for all the repeated experiments. It is worth noting that our graphene sensing substrate is fabricated based on pristine graphene layers, which are known to have better optical and electronic properties in comparison to the layers obtained by self-assembly of graphene oxides (GOs). The higher electron transfer rate and higher optical transparency of our pristine graphene sensing substrate also lead to a much stronger plasmon enhancement effect that resulted in extreme singularities in phase of reflected light of the metasurface. Further studies will be required to evaluate the designed system for detecting a series of aromatic ring structure biomolecules ranging from vitamins to helical peptides. As shown in Figures S10 and S11 (Supporting Information), proteins adsorbed on the graphene surface through pi-stacking interactions still maintain their biological activities such as catalytic activity of the enzyme. We envision that the reported sensing configuration will play an important role in designing future high-throughput multisensing platforms for clinical diagnostics of human diseases such as cancers. For example, our system will be able to sense cysteine-rich intestinal protein (CRIP) at $\times 10^{-18}$ M level, a 8.5 kDa protein that has been identified as an useful biomarker for detecting early stages of human breast cancer, cervical cancer, and pancreatic cancer.[35]

Supporting Information

Supporting Information is available from the Wiley Online Library or from the author.

Acknowledgements

This work was supported by the Singapore Ministry of Education (Grant Nos. Tier 2 MOE2010-T2-2-010 (M4020020.040 ARC2/11) and Tier 1 M4010360.040 RG29/10), NTU-NHG Innovation Collaboration Grant (No. M4061202.040), A*STAR Science and Engineering Research Council (No. M4070176.040), and School of Electrical and Electronic Engineering at NTU.

Received: April 13, 2015
Revised: August 3, 2015
Published online: September 9, 2015

[1] S. Zeng, D. Baillargeat, H.-P. Ho, K.-T. Yong, *Chem. Soc. Rev.* **2014**, *43*, 3426.
[2] A. V. Kabashin, P. Evans, S. Pastkovsky, W. Hendren, G. A. Wurtz, R. Atkinson, R. Pollard, V. A. Podolskiy, A. V. Zayats, *Nat. Mater.* **2009**, *8*, 867.
[3] P. Zijlstra, P. M. R. Paulo, M. Orrit, *Nat. Nanotechnol.* **2012**, *7*, 379.
[4] B. Liedberg, C. Nylander, I. Lundstrom, *Sens. Actuators, B* **1983**, *4*, 299.
[5] J. Homola, *Surface Plasmon Resonance Based Sensors*, Springer, Berlin, Germany **2006**.
[6] J. N. Anker, W. P. Hall, O. Lyandres, N. C. Shah, J. Zhao, R. P. Van Duyne, *Nat. Mater.* **2008**, *7*, 442.
[7] V. G. Kravets, F. Schedin, R. Jalil, L. Britnell, R. V. Gorbachev, D. Ansell, B. Thackray, K. S. Novoselov, A. K. Geim, A. V. Kabashin, A. N. Grigorenko, *Nat. Mater.* **2013**, *12*, 304.
[8] P. N. Prasad, *Introduction to Nanomedicine and Nanobioengineering*, Wiley, Hoboken, NJ **2012**.
[9] M. A. Cooper, *Nat. Rev. Drug Discovery* **2002**, *1*, 515.
[10] A. V. Kabashin, P. I. Nikitin, *Quantum Electron.* **1997**, *27*, 653.
[11] H. P. Ho, W. W. Lam, *Sens. Actuators, B* **2003**, *96*, 554.
[12] Y. Huang, H. P. Ho, S. K. Kong, A. V. Kabashin, *Ann. Phys.* **2012**, *524*, 637.
[13] A. V. Kabashin, S. Patskovsky, A. N. Grigorenko, *Opt. Express* **2009**, *17*, 21191.
[14] N. I. Zheludev, Y. S. Kivshar, *Nat. Mater.* **2012**, *11*, 917.
[15] A. N. Grigorenko, M. Polini, K. S. Novoselov, *Nat. Photonics* **2012**, *6*, 749.
[16] Q. L. Bao, K. P. Loh, *ACS Nano* **2012**, *6*, 3677.
[17] H. Yan, T. Low, F. Guinea, F. Xia, P. Avouris, *Nano Lett.* **2014**, *14*, 4581.
[18] R. Verma, B. D. Gupta, R. Jha, *Sens. Actuators, B* **2011**, *160*, 623.
[19] P. Wang, O. Liang, W. Zhang, T. Schroeder, Y.-H. Xie, *Adv. Mater.* **2013**, *25*, 4918.
[20] L. Wu, H. S. Chu, W. S. Koh, E. P. Li, *Opt. Express* **2010**, *18*, 14395.
[21] B. Song, D. Li, W. P. Qi, M. Elstner, C. H. Fan, H. P. Fang, *Chem. Phys. Chem.* **2010**, *11*, 585.
[22] S. Akca, A. Foroughi, D. Frochtzwajg, H. W. C. Postma, *PLoS One* **2011**, *6*, e18442.
[23] W. C. Law, K. T. Yong, A. Baev, P. N. Prasad, *ACS Nano* **2011**, *5*, 4858.
[24] M. J. Kwon, J. Lee, A. W. Wark, H. J. Lee, *Anal. Chem.* **2012**, *84*, 1702.
[25] A. V. Kildishev, A. Boltasseva, V. M. Shalaev, *Science* **2013**, *339*, 1232009.
[26] N. Yu, F. Capasso, *Nat. Mater.* **2014**, *13*, 139.
[27] I. Pockrand, *Surf. Sci.* **1978**, *72*, 577.
[28] P. K. Jain, K. S. Lee, I. H. El-Sayed, M. A. El-Sayed, *J. Phys. Chem. B* **2006**, *110*, 7238.
[29] G. Giovannetti, P. A. Khomyakov, G. Brocks, V. M. Karpan, J. van den Brink, P. J. Kelly, *Phys. Rev. Lett.* **2008**, *101*, 026803.
[30] R. R. Nair, P. Blake, A. N. Grigorenko, K. S. Novoselov, T. J. Booth, T. Stauber, N. M. R. Peres, A. K. Geim, *Science* **2008**, *320*, 1308.
[31] S. H. Choi, Y. L. Kim, K. M. Byun, *Opt. Express* **2011**, *19*, 458.
[32] H. Zhang, Y. Sun, S. Gao, J. Zhang, H. Zhang, D. Song, *Small* **2013**, *9*, 2537.
[33] Y. Lu, S. Peng, D. Luo, A. Lal, *Nat. Commun.* **2011**, *2*, 578.
[34] S. Zeng, K.-T. Yong, I. Roy, X.-Q. Dinh, X. Yu, F. Luan, *Plasmonics* **2011**, *6*, 491.
[35] J. Hao, A. W. R. Serohijos, G. Newton, G. Tassone, Z. Wang, D. C. Sgroi, N. V. Dokholyan, J. P. Basilion, *PLoS Comput. Biol.* **2008**, *4*, e1000138.